Received: *February 8, 1999,* Accepted: *March 25, 1999*

Gap equation in finite-temperature three-dimensional QED beyond the bare-vertex approximation

George Triantaphyllou*

Institut für Theoretische Physik, Technische Universität München
James-Franck-Strasse, D-85748 Garching, Germany
E-mail: georg@physik.tu-muenchen.de

Abstract: Dynamical mass generation in a three-dimensional version of finite-temperature QED is studied with the help of Schwinger-Dyson equations in the real-time formalism. We go beyond the bare-vertex approximation and include wave-function renormalization effects. This introduces a system of two integral equations which are solved numerically. In order to increase the reliability of the results, fermion and photon self-energies varying independently with energy and momentum are used. The method applied enables a detailed study of the behaviour of the theory with increasing temperature and number of fermion flavours.

Keywords: Thermal Field Theory, Field Theories in Lower Dimensions.

*Alexander von Humboldt fellow

JHEP03(1999)020

Contents

1. Introduction **1**

2. Taking wave-function renormalization into account **2**

3. Solving the system of equations **5**
- 3.1 The algorithm 5
- 3.2 Behaviour of the theory with temperature 6
- 3.3 Behaviour of the theory with the number of fermion flavours 9

4. Conclusions **12**

1. Introduction

Three-dimensional QED can exhibit interesting non-perturbative phenomena like dynamical mass generation [1]–[3]. A finite-temperature version of the theory, referred to sometimes as τ_3-QED, has been suggested to be relevant to high-temperature superconductivity [4]. The critical behaviour of the theory with varying temperature T and number of fermion flavours N_f was recently studied numerically in the Schwinger-Dyson formalism [5]. In that paper, a bare-vertex approximation was used in the gap equation for the fermion self-energy Σ, and wave-function renormalization was neglected. These approximations correspond to a particular truncation of the Schwinger-Dyson hierarchy and to the simplest way of making this scheme useful for computations. Since this could influence the final results, we return to the problem in order to study the impact of these approximations. Their potential importance has been stressed in [6], especially in connection with the behaviour of the theory when the number of fermion flavours is varied. This has led to several interesting studies at zero-temperature trying to include these effects [7]–[9], in order to solve the controversy on whether there is a critical number of fermion flavours beyond which there is no mass generation. At finite temperature, similar studies have so far used several approximations that we will relax in this study.

The first goal of this paper is to give an estimate for the ratio $r = 2M(0,0)/k_B T_c$ [4] that is free from severe approximations used frequently in the past. Here $M(0,0)$ is the fermion mass function at zero momentum and energy and T_c is the critical temperature beyond which there is no mass generation. Apart from being theoretically very interesting, this quantity is of direct physical relevance since it can be compared to corresponding values measured in certain high-temperature superconductors. The second goal is to provide a reliable phase diagram of the theory with respect to T and N_f. In order to achieve these goals, the bare-vertex approximation is here relaxed and wave-function renormalization is taken into account.

This complicates the study considerably and constitutes a non-trivial step forward, since instead of having only one gap equation, a system of two integral equations has to be solved. In particular, the numerical algorithm becomes more complicated than before and each iteration requires more computing time. As in [5] however, we continue to work with fermion and photon self-energies varying independently with energy and momentum, something which by itself is a very important improvement of similar investigations in the past [10]. We continue to neglect the imaginary parts of the photon polarization functions and of the fermion self-energy for simplicity, as other studies have done so far [10]–[12]. A more detailed treatment would of course involve the full propagators [13], but this is left to future studies due to the limited numerical accuracy of the present method.

2. Taking wave-function renormalization into account

The study of the fermion self-energy and mass function in a non-perturbative context is central to our study, and the Schwinger-Dyson formalism will provide the basis of this investigation. The Schwinger-Dyson equation for the fermion self-energy is given by

$$S^{-1}(p) = S_0^{-1}(p) - e^2 \int \frac{d^3k}{(2\pi)^3} \gamma^\mu S(q) \Delta_{\mu\nu}(k) \Gamma^\nu(p,q)\,, \tag{2.1}$$

where $q = p - k$, e is the dimensionful gauge coupling of the theory which we will take to be constant throughout this paper, $\Delta_{\mu\nu}$ is the photon propagator with $\mu, \nu = 0, 1, 2$, Γ^ν is the full photon-fermion vertex, γ^μ is a four-dimensional representation of the γ-matrices, S_0 is the bare fermion propagator, and the finite-temperature fermion propagator in the real-time formalism is given by

$$\begin{aligned} S(p) = \Big((1 + A(p))\, \not{p} + \Sigma(p)\Big) \Bigg(& \frac{1}{(1 + A(p))^2\, p^2 + \Sigma^2(p)} - \\ & - \frac{2\pi\delta((1 + A(p))^2 p^2 + \Sigma^2(p))}{e^{\beta|p_0|} + 1} \Bigg)\,, \end{aligned} \tag{2.2}$$

where $\beta = 1/k_B T$, $A(p)$ is the wave-function renormalization function, δ is the usual Dirac function and we have made a rotation to Euclidean space. Note that we avoid the matrix form that the propagator has in this formalism, since the Schwinger-Dyson equation that we have written down involves only a one-loop diagram directly, so complications due to the field-doubling problem do not arise [14]. Moreover, due to the broken Lorenz invariance at finite temperature, the wave function renormalization could in principle affect differently the p_0 and $|\vec{p}|$ propagator components, i.e. we should replace $(1+A(p))\not{p}$ by $((1+A(p))\gamma^0+a)p_0+(1+B(p))\gamma^i p_i$ with $i=1,2$. For simplicity we will restrict ourselves to situations where $a=0$, which correspond to a zero chemical potential, and we will work in the approximation where $A(p)=B(p)$ also for non-zero temperatures as done in similar studies [12] for simplicity, even though there is no *a priori* justification for this. We will return to this matter later.

For the vertex $\Gamma^\nu(p,q)=\Gamma_A(p,q)\gamma^\nu$ we use two different ansätze, where we take $\Gamma_A(p,q)$ to be equal to $1+A(q)$ or to the symmetrized one $1+\left(A(p)+A(q)\right)/2$, and $A(q)$ is the same wave-function renormalization function appearing in the fermion propagator. Even though these vertices do not satisfy *a priori* the Ward-Takahashi identities, they are expected to incorporate the basic qualitative features of a non-perturbative vertex at zero temperature when used in a Schwinger-Dyson context [15]. The first choice has been used in a finite-temperature case [12], supported by the qualitative agreement of the results of this ansatz with the ones obtained by more elaborate treatments [6]. The second vertex is discussed in ref. [16] and we will refer to it as the symmetric vertex. Even though these choices correspond to specific truncations of the Schwinger-Dyson hierarchy, they expected to give qualitatively reliable results.

Moreover, the photon propagator in the Landau gauge is given by [4]

$$\Delta_{\mu\nu}(k)=\frac{Q_{\mu\nu}}{k^2+\Pi_L(k)}+\frac{P_{\mu\nu}}{k^2+\Pi_T(k)}\,, \tag{2.3}$$

where

$$\begin{aligned} Q_{\mu\nu} &= \left(\delta_{\mu 0}-\frac{k_\mu k_0}{k^2}\right)\frac{k^2}{\vec{k}^2}\left(\delta_{\nu 0}-\frac{k_\nu k_0}{k^2}\right) \\ P_{\mu\nu} &= \delta_{\mu i}\left(\delta_{ij}-\frac{k_i k_j}{\vec{k}^2}\right)\delta_{\nu j} \end{aligned} \tag{2.4}$$

with $i,j=1,2$, and where we neglect its temperature-dependent delta-function part since it is expected to give a vanishingly small contribution [5, 11, 17]. The longitudinal and transverse photon polarization functions Π_L and Π_T are given in [11], where they are calculated in a massless-fermion approximation. Note that in principle one should also have an integral equation for the polarization functions coupled to M and A, but this would complicate this study even numerically too much, and we therefore continue to work with this approximation.

Identifying the parts of this equation with the same spinor structure, we reduce the problem to that of a system of two three-dimensional integral equations involving two functions varying independently with p_0 and $|\vec{p}|$.

The equations take the following form:

$$
\begin{aligned}
M(p_0,|\vec{p}|) = {} & \frac{\alpha}{N_f(1+A(p_0,|\vec{p}|))}\int\frac{dk_0|\vec{k}|d|\vec{k}|d\theta}{(2\pi)^3}\frac{M(q_0,|\vec{q}|)R(p_0,|\vec{p}|,q_0,|\vec{q}|)}{q^2+M^2(q_0,|\vec{q}|)}\times \\
& \times\sum_{P=L,T}\frac{1}{k^2+\Pi_P(k_0,|\vec{k}|)}- \\
& -\frac{\alpha}{N_f(1+A(p_0,|\vec{p}|))}\int\frac{|\vec{k}|d|\vec{k}|d\theta}{(2\pi)^2}\frac{M(E,|\vec{q}|)R(p_0,|\vec{p}|,E,|\vec{q}|)}{2E(e^{\beta E}+1)}\times \\
& \times\sum_{\epsilon=1,-1}\sum_{P=L,T}\frac{1}{(p_0-\epsilon E)^2+\vec{k}^2+\Pi_P(p_0-\epsilon E,|\vec{k}|)} \\
A(p_0,|\vec{p}|) = {} & \frac{\alpha}{N_fp^2}\int\frac{dk_0|\vec{k}|d|\vec{k}|d\theta}{(2\pi)^3}\frac{R(p_0,|\vec{p}|,q_0,|\vec{q}|)}{q^2+M^2(q_0,|\vec{q}|)}\times \\
& \times\left(\frac{Q(p_0,\vec{p},k_0,\vec{k})}{k^2+\Pi_L(k_0,|\vec{k}|)}+\frac{P(p_0,\vec{p},k_0,\vec{k})}{k^2+\Pi_T(k_0,|\vec{k}|)}\right)- \\
& -\frac{\alpha}{N_fp^2}\int\frac{|\vec{k}|d|\vec{k}|d\theta}{(2\pi)^2}\frac{R(p_0,|\vec{p}|,E,|\vec{q}|)}{2E(e^{\beta E}+1)}\times \\
& \times\sum_{\epsilon=1,-1}\left(\frac{Q(p_0,\vec{p},p_0-\epsilon E,\vec{k})}{(p_0-\epsilon E)^2+\vec{k}^2+\Pi_L(p_0-\epsilon E,\vec{k})}+\right. \\
& \left.+\frac{P(p_0,\vec{p},p_0-\epsilon E,\vec{k})}{(p_0-\epsilon E)^2+\vec{k}^2+\Pi_T(p_0-\epsilon E,\vec{k})}\right),
\end{aligned}
\tag{2.5}
$$

where $\alpha = e^2N_f$, $R(p_0,|\vec{p}|,q_0,|\vec{q}|) = \frac{\Gamma_A(p_0,|\vec{p}|,q_0,|\vec{q}|)}{1+A(q_0,|\vec{q}|)}$, and it is more convenient to work with the mass function $M(p_0,|\vec{p}|) = \Sigma(p_0,|\vec{p}|)/(1+A(p_0,|\vec{p}|))$. The function R is obviously equal to the identity for the first vertex choice. We also sum over the photon polarizations $P = L, T$ and over the two roots of the delta function by introducing $\epsilon = 1, -1$. The quantity E is approximated by the relation $E^2 \approx |\vec{q}|^2 + M^2(0,0)$ [5], where use of the delta-function property $\delta(ax) = \delta(x)/|a|$ has been made.

Furthermore, the functions Q and P are given by

$$
\begin{aligned}
Q(p_0,\vec{p},k_0,\vec{k}) &= 2\left(p_0-\frac{(pk)k_0}{k^2}\right)\frac{k^2}{\vec{k}^2}\left(q_0-\frac{(qk)k_0}{k^2}\right) \\
P(p_0,\vec{p},k_0,\vec{k}) &= 2\left(\vec{p}\,\vec{q}-\frac{(\vec{p}\vec{k})(\vec{k}\vec{q})}{\vec{k}^2}\right)-pq.
\end{aligned}
\tag{2.6}
$$

One can easily check that $Q+P = -2(pk)(kq)/k^2$, which would reproduce the result of [12] if one takes $\Pi_L(k) = \Pi_T(k) = \Pi(k)$ and switches to imaginary-time formalism (note that our q has the opposite sign than the one in [12]).

The equations for $M(p_0, |\vec{p}|)$ and $A(p_0, |\vec{p}|)$ have to be solved self-consistently, and the equation for the mass function actually always accepts, apart from the solutions we will seek, the trivial solution as well. An analytical study of such a system would not be possible without severe approximations, so we proceed to the numerical solution of the equations given above.

3. Solving the system of equations

3.1 The algorithm

In order to attack the problem numerically, we have to discretize our momentum space. The technique will in principle be similar to the one in [5], but the algorithm will be substantially complicated due to the fact that we now have to solve a system of two four-dimensional integral equations involving functions of two variables. The gap equations are both ultraviolet (UV) and infrared (IR) finite, with α providing an effective UV cut-off [2] and the fermion mass function providing a physical IR cut-off. Therefore, we use UV and IR cut-offs Λ_{IR} and Λ_{UV} only for numerical reasons. However, we are always careful to keep the temperature T and the mass function M within the range of Λ_{IR} and Λ_{UV}. It is a well-known problem however that the existence of this IR cut-off does not allow us to draw firm conclusions on the criticality of the theory, since a mass function dropping below this cut-off could be small but still not exactly zero. We will return to this issue later. The complexity of the algorithm does not allow us to consider $\Lambda_{IR}/\Lambda_{UV}$ ratios smaller than 10^{-4}. Since the momentum space spans several orders of magnitude, we use logarithmic variables and discretize the squares of external and loop momenta according to $\log_{10}(\Lambda_{IR}^2) + \frac{i}{n}\log_{10}(\Lambda_{UV}^2/\Lambda_{IR}^2)$, and the integration angle θ according to $2\pi i/n$, where $i = 1, \ldots, n$. We have therefore a five-dimensional lattice, with three dimensions coming from the integrals and two from the external momenta.

The results presented in this paper are for a lattice having 16 points in each of the five dimensions. We checked the stability of our results for lattices of other sizes as well, although computing-time limitations did not allow us to consider much larger lattices. We then use a relaxation method described in ref.[5] to solve our system of equations self-consistently by iterations. We do not exceed a 10% numerical accuracy of the results in the worst cases, which we judge as satisfactory due to the complexity of the algorithm. We trace back this numerical uncertainty to the minimum achievable root-mean-square deviation of the input and output configurations of the algorithm. This deviation is much smaller if one neglects the high-momentum regions where the solutions are vanishingly small and where numerical errors appear easier. Note however that the mean relative difference of the input and output configurations is monotonically decreasing with each iteration, like the deviation, but reaches values as low as 10^{-4}, which we consider as an indication of an overall convergence. On the contrary, in non-converging cases this difference is increasing and the configurations tend rapidly to zero, apart from the fact that the deviation is oscillating randomly taking sometimes unusually large values. We therefore have a clear-cut convergence criterium to enable us to study the critical behaviour of the theory.

3.2 Behaviour of the theory with temperature

The solution at $T = 0$ and $N_f = 2$ for the functions $\Sigma(p_0, |\vec{p}|)$ and $-A(p_0, |\vec{p}|)$ for the vertex with $\Gamma_A(p,q) = 1 + A(q)$ is given in figs. 1 and 2 respectively. The general form of these functions does not change with increasing temperature, varying of N_f or by using the symmetric vertex instead. The function $\Sigma(p_0, |\vec{p}|)$ falls as expected with increasing momentum, and is of the same form as the mass function $M(p_0, |\vec{p}|)$. The function $A(p_0, |\vec{p}|)$ is always in the range between -1 and 0 as required [18], it is tending to zero for increasing momenta, and it is of the same form and magnitude as the approximate form used in [12]. In view of the approximation $A(p) = B(p)$ for the wave-function renormalization stated at the beginning, the roughly symmetric behaviour of the two functions A and Σ with respect to p_0 and $|\vec{p}|$ argues in support for the self-consistency of the calculation. Moreover, the low-momentum values of the wave-function renormalization, which are on the order of $A(0,0) \approx -0.3$, indicate the importance of including its effects in a complete calculation in this gauge.

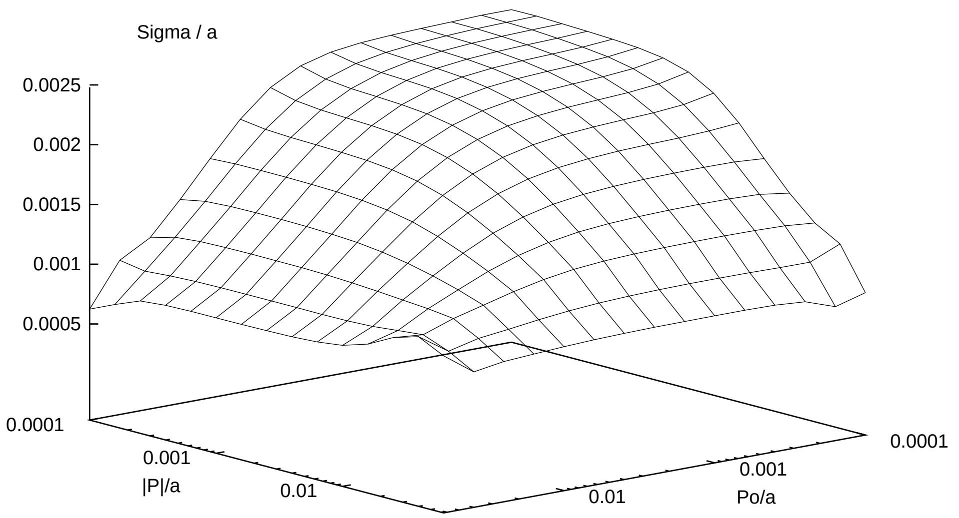

Figure 1: The fermion self-energy $\Sigma(p_0, |\vec{p}|)$ at zero temperature and for $N_f = 2$, $\Lambda_{UV}/\alpha = 0.1$, as a function of energy and momentum in logarithmic scale. All quantities are scaled by α.

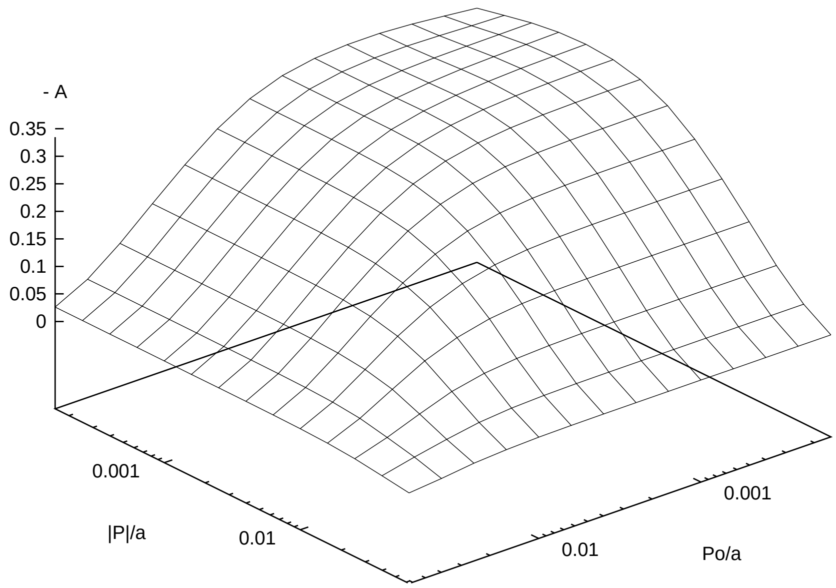

Figure 2: The opposite of the wave-function renormalization $-A(p_0, |\vec{p}|)$ at zero temperature and for $N_f = 2$, $\Lambda_{UV}/\alpha = 0.1$.

For a given number of fermion flavours N_f, when the temperature exceeds some critical value there is no solution for the fermion mass function but the trivial one. We infer that not only by the fact that the relaxation algorithm does not converge, but also because the output configurations tend rapidly to zero and after a number of iterations they fall below the IR cut-off. One should note that the temperature at which this happens could be somewhat smaller than the critical one, since the zero-momentum mass function at slightly smaller temperatures is not very much smaller than the one at zero temperature. The abrupt fall of the solution with temperature thus could possibly be an indication that the initial smooth input configuration is unable to converge to the correct solution, which is rapidly varying but still not zero. Since the dimensionless ratio r of (twice) the zero-momentum and zero-temperature fermion mass function divided by this critical temperature is important for the study of solid-state systems, we list in tables 1 and 2 its values for various choices of N_f and Λ_{UV}/α, for our two different choice of vertices. Note that the case $N_f = 2$ is the one relevant to high-temperature superconductivity.

The fermion mass function falls with increasing momenta and the results obtained should not depend on the choice of the UV cut-off. Even though the limited number of lattice points did not allow us to explore the region $\Lambda_{UV} > \alpha$, this is not expected to be physically interesting since the critical temperature and the fermion mass function is always orders of magnitude smaller than α. For the same reason, we tend to trust more our results with lower Λ_{UV}/α ratios, since then the lattice

Fermion flavours $\Rightarrow$	$N_f = 1$			$N_f = 2$			$N_f = 3$		
Λ_{UV}/α $\Downarrow$	m_o	t_c	r	m_0	t_c	r	m_0	t_c	r
0.1	21	4.5	9.4	3.3	0.6	11.0	0.65	0.12	10.6
0.5	32	6.2	10.4	4.0	0.72	11.1	1.3	0.26	10.0
1	32	6.1	10.5	4.4	0.75	11.7	1.4	0.27	10.4

Table 1: The quantities $m_0 = 10^3 \times M(0,0)/\alpha$ at $T = 0$, $t_c = 10^3 \times k_B T_c/\alpha$ and $r = 2m_0/t_c$ for different values of flavours and ultra-violet cut-offs Λ_{UV}. The vertex with $\Gamma_A(p,q) = 1 + A(q)$ is used.

Fermion flavours $\Rightarrow$	$N_f = 1$			$N_f = 2$			$N_f = 3$		
Λ_{UV}/α $\Downarrow$	m_o	t_c	r	m_0	t_c	r	m_0	t_c	r
0.1	22	4.6	9.6	3.4	0.67	10.1	1.1	0.21	10.5
0.5	29	5.7	10.2	4.7	0.85	11.1	1.4	0.27	10.4
1	31	5.8	10.7	5.0	0.9	11.1	1.5	0.28	10.7

Table 2: The same quantities as table 1 using the symmetric vertex.

spacing becomes smaller and the integrations more accurate. At momenta of order $\Lambda_{UV} = 0.1\alpha$ the mass function is already negligibly small, and thus our results are not influenced by such a UV cut-off. We were not able to consider even smaller Λ_{UV}/α as in [5] due to numerical problems caused by the complexity of the algorithm.

We note that in general the value of r remains roughly stable for various choices for N_f and Λ_{UV}. It is in fact more stable than the r ratio computed in [5], which could be an indication that the wave-function renormalization $A(p_0, |\vec{p}|)$ plays a -at least numerically- stabilizing role in the system under study. In this respect, the results presented here could be more trustworthy. Furthermore, comparing the tables 1 and 2 one can see that the r-ratio is not considerably affected by the particular choice of our vertices. Moreover, we note that its value is concentrated approximately around $r \approx 10.7$, which is comparable to the values obtained in [5] which neglected $A(p_0, |\vec{p}|)$. The ratio r found is also comparable to typical values obtained in ref. [12], which includes wave-function renormalization effects but uses several approximations which we were able to by-pass in this study. We confirm therefore that adding these effects does not influence the behaviour of the theory in a significant way. We have to note moreover that our r values are somewhat larger than the value $r \approx 8$ measured for some high-temperature superconductors [19]. However, as already discussed, we could be overestimating this ratio because of a possibly poor convergence of the algorithm for temperatures close to the critical one.

3.3 Behaviour of the theory with the number of fermion flavours

At zero-temperature, this theory is known to exhibit also an interesting behaviour with the number of fermions N_f. In fig. 3 we plot the zero-momentum and zero-temperature fermion mass function with respect to N_f, fitted with the same exponential curve for both vertices, since their behaviour is similar. There are two reasons why we do not try to fit them with a function non-analytic in N_f, as was done in [5]. One reason is that the non-analytic form used before and predicted by some studies is expected to be valid only for a number of fermion flavours close to a possibly critical value N_c, so efforts to use the same functional form for N_f away from this value could give a misleading value for N_c. The other is that our present results for the ratio r seem to be quite stable with N_f, and we would like to be able to estimate in a simple way some sort of "mean" r-ratio by combining these data with the ones showing the T_c dependence on N_f, as will be described below.

At $N_f \approx 3.35$, the mass function is still roughly four times larger than the cut-off. When $N_f \gtrsim 3.35$, our algorithm does not converge and the mass function tends fast below the IR cut-off. Note that this value did not vary substantially for different choices of Λ_{IR} or the vertex. This behaviour could indicate that $N_f \approx 3.35$ is some critical point beyond which dynamical mass generation is impossible. However,

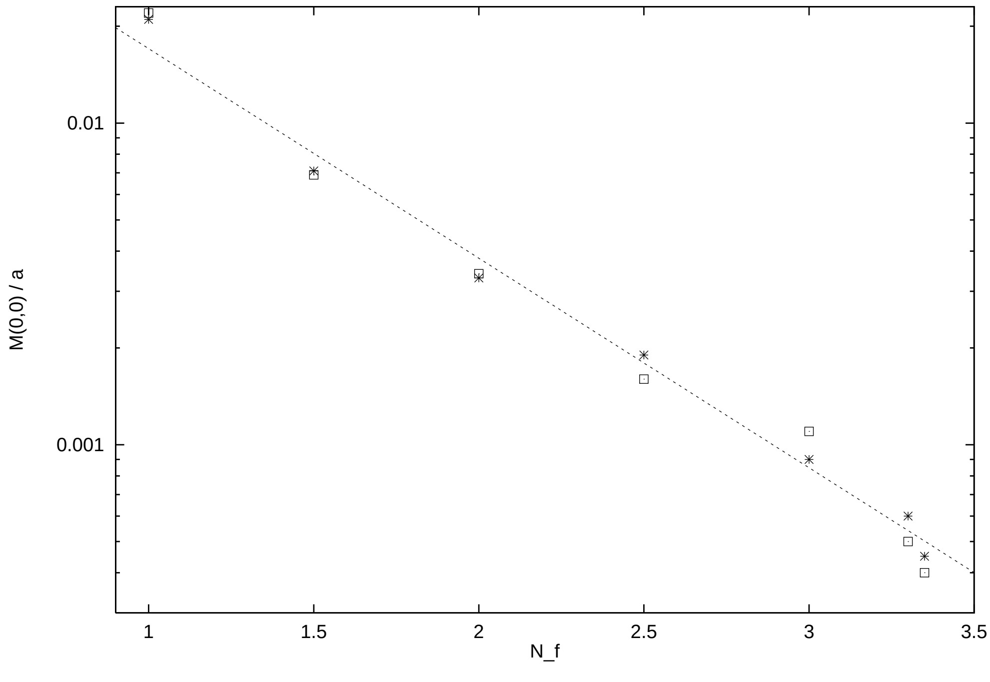

Figure 3: The fermion mass function at zero momentum and zero temperature, scaled by α and on a logarithmic scale, with respect to N_f for a ratio $\Lambda_{UV}/\alpha = 0.1$. Stars and squares correspond to the vertex with $\Gamma_A = 1 + A(p)$ and the symmetric vertex respectively. We fit our results for both vertices with the curve $M(0,0)/\alpha = e^{-1.5N_f}/13.1$. Values of N_f larger than 3.35 are not considered, because then the self-energy falls below the IR-cut-off.

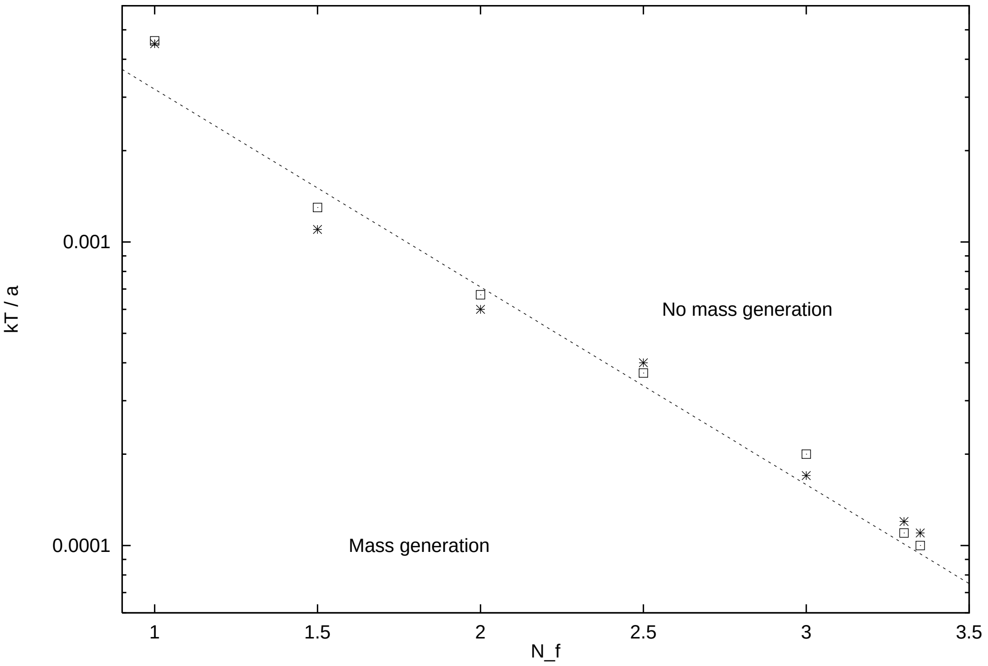

Figure 4: The phase diagram of the theory with respect to the temperature scaled by α and in logarithmic scale and the number of fermion flavours, for a ratio $\Lambda_{UV}/\alpha = 0.1$. Stars and squares correspond to the vertex with $\Gamma_A = 1 + A(p)$ and the symmetric vertex respectively. We fit the data points with the curve $k_B T/\alpha = e^{-1.5N_f}/70$. This curve should not be extrapolated for $N_f \gtrsim 3.35$.

numerical limitations did not allow us to explore the region $\Lambda_{IR} < 10^{-4}\Lambda_{UV}$. In other words, if there were a solution for the mass function smaller than roughly $10^{-4}\Lambda_{UV}$, our algorithm would not be able to find it because it would fall below the IR cut-off. The finite size of our lattice therefore does not allow us to draw firm conclusions on the matter, and the fitting curve should not be extrapolated beyond this limiting N_f value.

The value of N_f where this behaviour comes in effect is remarkably close to the one quoted in the numerical study of [9], and it is also close to our previous result [5]. These values are however roughly 25% smaller than the one quoted in the theoretical studies of refs. [20], [21] which take wave-function renormalization effects into account. A similar study [7], which includes a calculation of the fermion-field anomalous dimension to second-order in $1/N_f$, predicts a critical value $N_f \approx 3.28$, which is only slightly larger than the theoretical prediction neglecting wave-function renormalization which gives $N_f = 32/\pi^2 \approx 3.24$ [2], and quite close to the value where our algorithm looses convergence.

In fig. 4 we plot the phase diagram of the theory with respect to N_f and $k_B T$. It separates two regions of the parameter space which either allow or do not allow dynamical mass generation. The approximate stability of r with increasing N_f lead us to rescale the data points of this plot and fit these simultaneously with the data points of fig. 3, with the same exponential curve $e^{-1.5N_f}/13.1$ for both vertices, since they exhibit a similar behaviour. The slope of this exponential fits also relatively well the data on the two plots separately, even though the slope of the exponential of the mass function separately is closer to -2. It is however lower in absolute value than the one reported in [15] . We note also that the fall of the critical temperature with the number of fermion flavours is slower than in [5], which was found to be -2.5. The fast fall in that reference was the cause of the increase of the r-ratio with N_f, and we interpret it as poor convergence of that algorithm with large N_f values, because then the self-energy becomes smaller and more vulnerable to instabilities coming from numerical errors. The (double of the) rescaling factor was found to be $\bar{r} = 2M(0,0)/k_BT \approx 10.7$ and provides some kind of "mean" r-ratio which is independent of N_f. Its approximate value could actually be guessed by the data in tables 1 and 2.

The choice of an exponential fitting curve was only made to describe "phenomenologically" the general tendency of the data and to provide a measure for a r-ratio independently of N_f, and is reminiscent of the results in ref. [6] but with a steeper slope. However, there are also studies that predict a non-analytic behaviour of Σ for N_f near its critical value [2]. One could speculate that such a behaviour comes into effect also for our larger N_f data, since the slope of a curve connecting the large-N_f points of both figs. 3 and 4 is larger than the one of the general fit. Moreover, as already noted, near these N_f values the mass function is still roughly a factor of four larger than the IR cut-off, so the value of N_f quoted cannot be easily argued to be just an artifact of the finite lattice size. Lack of convergence of the algorithm and fall of the mass function below the IR cut-off however do not allow us to test the precise behaviour of the theory near $N_f \approx 3.35$, and it is also clear that the fitting curves should not be extrapolated for N_f larger than this value.

We remind the reader that the results quoted above were obtained with a photon propagator in the Landau gauge, which is convenient and widely used for this type of calculation. In addition, it possibly enables the wave-function renormalization to play a stabilizing role in the numerical algorithm and provide more accurate results. Since the final answers should be gauge-invariant however, one should in principle check whether other gauges, with corresponding vertices consistent with the Ward-Takahashi identities, give the same answer. In particular, calculations in the non-local gauge [22] eliminate the wave-function renormalization dependence of the results, since $A(p) = 0$, which means that the ratio r or the possibly critical number of fermion flavours should not be influenced by $A(p)$. In such a case, however, a different vertex choice than ours should be made, so that it does not reduce to the bare one when $A(p) = 0$. In our study, therefore, it is the taking into account of the wave-function renormalization in conjunction with a non-bare vertex that could potentially lead to results different from [5].

4. Conclusions

To conclude, we were able to solve a system of two integral equations for the fermion mass function and wave-function renormalization for a finite-temperature version of three-dimensional QED, by applying a numerical relaxation technique. The results presented are of course specific to the dimensionality of the system under study and to the abelian character of the theory. Both functions as well as the photon self-energies are taken to be energy- and momentum-dependent, use of two different non-bare vertices is made, and this leads to a more accurate and detailed study of the criticality of the theory. One main result is a r-ratio of about 10.7, which is close to previous numerical studies, confirming that including wave-function renormalization, in conjunction with two different non-bare fermion-photon vertices, does not affect the theory in a significant way. The other important result is the existence of a possibly critical fermion flavour number of roughly 3.35, which is also consistent with some theoretical expectations and other numerical calculations. But the use of an IR cut-off does not allow the precise exploration of the possible criticality at this stage.

It should be stressed here that such an agreement could not be taken for granted *a priori*, in view of the seriousness of truncations and approximations used in the past. It is the first time that such a study drops most of the approximations applied so far and allows a reliable description of the behaviour of the theory. We estimate the numerical uncertainty for the values quoted, which comes mainly from the convergence criteria imposed, at about $\pm 10\%$. The specific truncations of the Schwinger-Dyson hierarchy chosen in this work could of course easily introduce an additional theoretical error of comparable magnitude. We also note that a larger lattice than the one we used could be expected to improve the convergence of the algorithm and help us understand the behaviour of the fermion mass function at regions even closer to the critical temperature and flavour number. Furthermore, it remains to be seen if the inclusion of the imaginary parts of the self-energies could influence these results considerably.

Acknowledgments

I thank B. Bergerhoff for useful discussions and N. Mavromatos for bringing relevant calculations in the non-local gauge to my attention. This research is supported by an *Alexander von Humboldt Fellowship.*

References

[1] R.D. Pisarski, *Phys. Rev.* **D 29** (1984) 2423;
T. Appelquist, M. Bowick, D. Karabali and L.C.R. Wijewardhana, *Phys. Rev.* **D 33** (1986) 3704;
E. Dagotto, J.B. Kogut and A. Kocic, *Phys. Rev. Lett.* **62** (1989) 1083;

E. Dagotto, A. Kocic and J.B. Kogut, *Nucl. Phys.* **B 334** (1990) 279;
D. Atkinson, P.W. Johnson and P. Maris, *Phys. Rev.* **D 42** (1990) 602.

[2] T. Appelquist, D. Nash and L.C.R. Wijewardhana, *Phys. Rev. Lett.* **60** (1988) 2575.

[3] V.P. Gusynin, V.A. Miranskii and A.V. Shpagin, *Phys. Rev.* **D 58** (1998) 085023, [hep-th/9802136].

[4] N. Dorey and N.E. Mavromatos, *Nucl. Phys.* **B 386** (1992) 614.

[5] G. Triantaphyllou, *Phys. Rev.* **D 58** (1998) 065006, [hep-ph/9801245].

[6] M.R. Pennington and D. Walsh, *Phys. Lett.* **B 253** (1991) 246;
D.C. Curtis, M.R. Pennington and D. Walsh, *Phys. Lett.* **B 295** (1992) 313.

[7] D. Nash, *Phys. Rev. Lett.* **62** (1989) 3024.

[8] V.P. Gusynin, A.H. Hams and M. Reenders, *Phys. Rev.* **D 53** (1996) 2227, [hep-ph/9509380]

[9] P. Maris, *Phys. Rev.* **D 54** (1996) 4049, [hep-ph/9606214].

[10] N. Dorey and N.E. Mavromatos, *Phys. Lett.* **B 266** (1991) 163;
I.J.R. Aitchison, N. Dorey, M. Klein-Kreisler and N.E. Mavromatos, *Phys. Lett.* **B 294** (1992) 91, [hep-ph/9207246].

[11] I.J.R. Aitchison, *Z. Physik* **C 67** (1995) 303.

[12] I.J.R. Aitchison and M. Klein-Kreisler, *Phys. Rev.* **D 50** (1994) 1068, [hep-ph/9402213].

[13] A.V. Smilga, *Phys. Rep.* **291** (1997) 1, [hep-ph/9612347];
P.A. Henning, *Phys. Rep.* **253** (1995) 235.

[14] N. P. Landsman and C.G. van Weert, *Phys. Rep.* **145** (1987) 145;
R. Kobes and G.W. Semenoff, *Nucl. Phys.* **B 260** (1985) 714; *Nucl. Phys.* **B 272** (1986) 329;
L. Dolan and R. Jackiw, *Phys. Rev.* **D 9** (1974) 3320.

[15] M.R. Pennington and S.P. Webb, BNL Report No. BNL-40886, 1988 (unpublished);
D. Atkinson, P.W. Johnson and M.R. Pennington, BNL Report No. BNL-41615, 1988 (unpublished).

[16] J.S. Ball and T.W. Chiu, *Phys. Rev.* **D 22** (1980) 2542.

[17] A. Kocic, *Phys. Lett.* **B 189** (1987) 449;
T.S. Evans and R.J. Rivers, *Z. Physik* **C 40** (1988) 293.

[18] See for instance C. Itzykson and J.-B. Zuber, *Quantum Field Theory*, McGraw-Hill 1985.

[19] Z. Schlesinger, R.T. Collins, D.L. Kaiser and F. Holtzberg, *Phys. Rev. Lett.* **59** (1987) 1958.

[20] K.-I. Kondo, T. Ebihara, T. Iizuka and E. Tanaka, *Nucl. Phys.* **B 434** (1995) 85.

[21] I.J.R. Aitchison, N. Mavromatos and D. Mc Neill, *Phys. Lett.* **B 402** (1997) 154, [hep-th/9701087].

[22] H. Georgi, E.H. Simmons and A.G. Cohen, *Phys. Lett.* **B 236** (1990) 183;
T. Kugo and M.G. Mitchard, *Phys. Lett.* **B 282** (1992) 162.

JHEP03(1999)020